Available online at www.sciencedirect.com

SciVerse ScienceDirect

Procedia CIRP 5 (2013) 61 – 65

www.elsevier.com/locate/procedia

The First CIRP Conference on Biomanufacturing

Development of a Pneumatically-Driven Robotic Forceps with a Flexible Wrist Joint

Daisuke Haraguchi[a,]*, Kotaro Tadano[a], Kenji Kawashima[a]

[a]*Tokyo Institute of Technology*, *4259Nagatsuta, Yokohama, 226-8503, Japan*

* Corresponding author. Tel.: +81-045-924-5485 ; fax: +81-045-924-5486 .*E-mail address*: haraguchi.d.aa@m.titech.ac.jp .

Abstract

The present paper describes a pneumatically-driven forceps manipulator for minimally-invasive robot surgery that has a simplified flexible wrist joint for easy fabrication, cost reduction and future miniaturization. The joint structure consists only of a machined spring, and four NiTi super-elastic wires fixed to the joint-end are actuated by pneumatic cylinders in push-pull motions. This mechanism realizes two degrees-of-freedom bending motions of the wrist joint and provides higher manipulation stiffness than other flexible joint mechanisms. Theoretical models of the proposed mechanism are developed; kinematic relation between joint positions and actuator displacements is described as a simple ideal continuum model, and dynamic model of the manipulator is described considering frictional and elastic forces of the joint mechanism. The joint position control system employs a cascade structure: the outer loop of the position control with dynamics compensation and the inner loop of the pneumatic force control. Performances of the joint position control are evaluated through elementary experiments, and effectiveness of the proposed joint mechanism is demonstrated.

Selection and/or peer-review under responsibility of Professor Mamoru Mitsuishi and Professor Paulo Bartolo

Keywords: Surgical robot; Forceps manipulator; Pneumatic drive; Flexible joint

1. Introduction

In robotic assisted minimally-invasive surgery (MIS), distal dexterity enhancement is a key technology to solve the problem on insufficient degree of freedom (DOF) of the conventional tools for MIS. Here the most critical issue is the mechanism of dexterous joints. Previous developments of miniaturized surgical manipulators, in most cases, employed rigid link mechanisms for their wrist joints[1][2]. Rigid link mechanisms certainly provide structural stiffness and good controllability for manipulation. However, from a practical viewpoint, the complicated structure due to a lot of miniaturized components may increase the cost of fabrication and maintenance. Therefore, simplification of distal joint mechanisms becomes an essential issue for enhanced practicality.

Elastic and continuum mechanisms were also studied and applied to bendable endoscopes[3][4] and tool guiding systems[5]. This type of mechanism has a great advantage of the structural simplicity; unlike rigid link mechanisms, extra small parts such as shafts, bearings and pulleys are not needed. Hence these are essentially suitable for practical use and miniaturization.

The authors focus on the advantage of flexible mechanisms for distal joints of robotic surgical manipulators. In the previous work, the authors proposed a flexible wrist mechanism using a machined spring as the main structure[6]. Wire-tendon actuation was employed, however, there was a risk of buckling of the central backbone due to the wire tensions. To eliminate the risk, in this work, push-pull actuation of super-elastic wires are employed for the spring joint. This idea is inspired by the multi-backbone continuum robot proposed by Simaan et al.[7]. Further simplification and stiffness enhancement of the structure are achieved by this mechanism.

Selection and/or peer-review under responsibility of Professor Mamoru Mitsuishi and Professor Paulo Bartolo

doi:10.1016/j.procir.2013.01.012

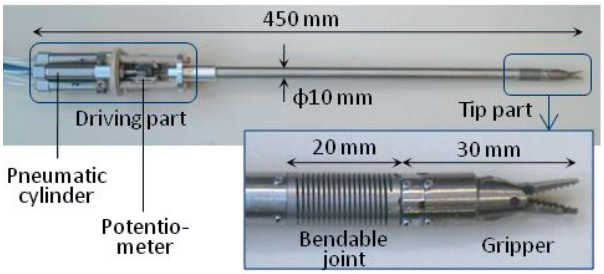

Fig.1 Overview of the forceps manipulator

In this work, the authors have developed a forceps manipulator using the proposed flexible mechanism for its wrist joint. Pneumatic actuators are employed for the robot because of their advantages: high power-to-weight ratio, high back-drivability for external force estimation[8], and a potential of MRI compatibility. Here are the contents of this paper. Section 2 describes hardware design of the forceps manipulator. Section 3 describes kinematic and dynamic modeling of the flexible joint. Section 4 describes the joint position controller and reports some experimental results of the position control. Section 5 describes conclusions and future works.

2. Design of the Forceps Manipulator

2.1. Overview

Fig.1 shows an overview of the forceps manipulator developed in this work. The diameter of insertion part into abdomen is 10 mm. The tip part has a two-DOF flexible wrist joint using a machined spring and a pneumatic gripper driven by air pressure[8]. This combination has the advantage that joint bending motions and gripping motions cannot interfere with each other. In the driving part, four pneumatic cylinders are equipped. The tip joint can bend in any direction by linear actuations of the cylinder rods through super-elastic wires connected to the joint. Positions of each cylinder rod are measured by linear potentiometers.

2.2. Structure of the flexible wrist mechanism

Fig.2 shows the detailed structures of each part in the manipulator. For the transmission of driving forces of the cylinders to the wrist joint, NiTi super-elastic wires (ϕ 0.6 mm) are employed. The wires are identically placed 90 degrees apart in a circle and connected to each cylinder rod and to the terminal of the wrist joint. Also, each wire is robustly supported by a stainless steel pipe in the long and thin body of the manipulator to prevent buckling of the wires. This structure enables push-pull actuation of the super-elastic wires to enhance the joint stiffness.

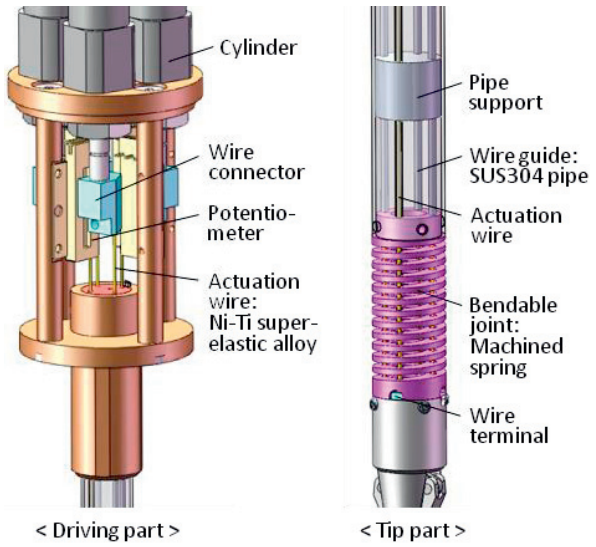

Fig.2 Mechanism design of the forceps manipulator

Furthermore, mechanical backlash of the driving system can be greatly reduced, compared with a system using conventional stranded wire ropes.

For the main structure of the flexible joint, a machined spring is employed. This spring component provides excellent torque transmissibility of the joint in contrast to its bending flexibility, which is a suitable characteristics for precise and stable manipulations. The machined spring is all the necessary component of the wrist joint because wire-guidance halls and other attachment parts can be integrally manufactured with the spring.

The number of components for the two-DOF bendable wrist mechanism can be minimized with the proposed structure. In particular, a central backbone to prevent compressions of the spring[6] is no longer necessary because “push” actuations are allowed with the proposed structure. Due to the structural simplicity with enhanced stiffness, this mechanism is widely applicable for other surgical tools requiring precise and stable manipulations.

2.3. Pneumatic driving system

The forceps manipulator performs two-DOF bending motions of the flexible wrist joint using four pneumatic cylinders. Fig.3 shows a schematic of the pneumatic driving system for one-DOF bending motion by paired two cylinders. Each cylinder is driven by a five-port-type servo valve, and pressure sensors are placed at each output port of the valves. In this system, a pneumatic driving force of *i*th cylinder F_i is calculated as follows:

$$F_i = A_{iu}P_{iu} - A_{i\ell}P_{i\ell} \tag{1}$$

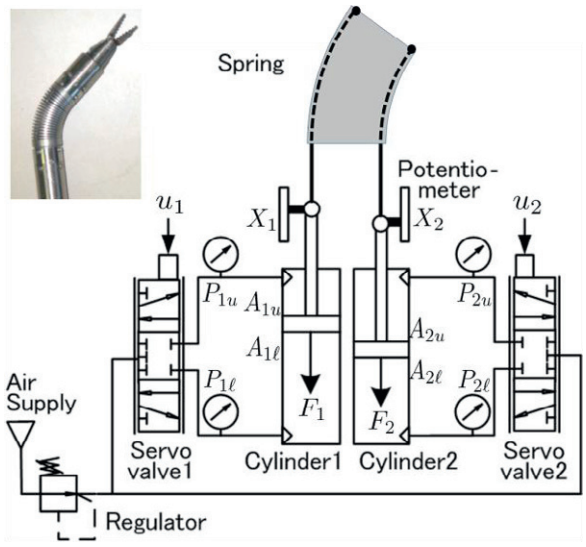

Fig.3 Schematic of the pneumatic driving system for one-DOF bending

where symbols A and P denote cross-sectional areas of the cylinders and pressures measured by the pressure sensors, respectively. In this work, dynamical effects of the pneumatic pipelines are not considered.

3. Theoretical Models of the Manipulator

3.1. Kinematic modeling

Kinematic relations between the wrist joint and the pneumatic cylinders are derived using a continuum model studied in the preceding work[9]. Fig.4 shows nomenclature and a reference coordinate frame on the flexible wrist joint. The reference frame is set at the center of the joint base, where $\boldsymbol{x}$ and $\boldsymbol{y}$ axes are set on the No.1 and the No.3 wires. A two-dimensional joint position vector $\boldsymbol{q}=[\delta,\theta]^T$ is defined, where δ denotes the bending direction and θ denotes the bending angle depicted in Fig.4. This model has two assumptions; first, the flexible joint bends into an ideal circular shape; second, the axial length of the joint denoted by L is constant ($L=20$ mm for this manipulator).

Under the conditions above, displacements of the four cylinder rods denoted by $\boldsymbol{X}$ (i.e., variations in the wire lengths of the joint part) can be geometrically expressed using the joint position parameters:

$$\boldsymbol{X}(\boldsymbol{q})=\begin{bmatrix}X_1\\X_2\\X_3\\X_4\end{bmatrix}=\begin{bmatrix}-r\theta\cos\delta\\-r\theta\sin\delta\\r\theta\cos\delta\\r\theta\sin\delta\end{bmatrix} \tag{2}$$

where r denotes the pitch circle radius on the wire locations ($r=3.6$ mm for this manipulator).

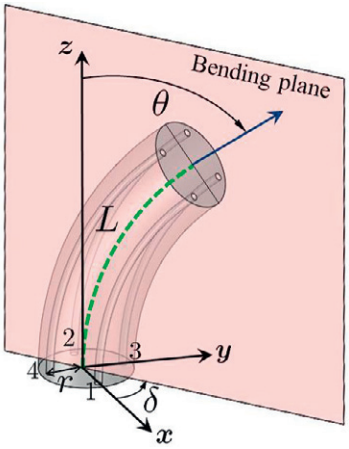

Fig.4 Nomenclature and a reference frame on the flexible joint

Solving equation (2) for the joint position $\boldsymbol{q}$ yields

$$\boldsymbol{q}(\boldsymbol{X})=\begin{bmatrix}\delta\\\theta\end{bmatrix}=\begin{bmatrix}\tan^{-1}\left(\dfrac{X_1-X_3}{X_2-X_4}\right)\\\dfrac{1}{2r}\sqrt{(X_1-X_3)^2+(X_2-X_4)^2}\end{bmatrix} \tag{3}$$

Actual joint position parameters are calculated by equation (3) with cylinder rod positions measured by the potentiometers.

3.2. Dynamic modeling

The manipulator dynamics are modeled at the level of the four pneumatic actuators as follows:

$$\boldsymbol{F}(\boldsymbol{q},\dot{\boldsymbol{X}})=\boldsymbol{C}\dot{\boldsymbol{X}}+\boldsymbol{D}\,\mathrm{sgn}(\dot{\boldsymbol{X}})e^{2\mu\theta}+\boldsymbol{K}(\boldsymbol{q}) \tag{4}$$

$\boldsymbol{F}$ in the left-hand side denotes pneumatic driving forces of the four cylinders, and the following are explanations of each term in the right-hand side.

The first term denotes viscous frictional forces of the pneumatic cylinders, where $\boldsymbol{C}$ is a constant and diagonal matrix of the viscosities. The second term denotes sliding frictional forces acting on the joint actuation mechanism, where $\boldsymbol{D}$ is a constant and diagonal matrix of the frictional forces. Since conditions of the sliding friction vary depending on the joint bending angle θ, a nonlinear coefficient $e^{2\mu\theta}$ is added based on the Euler's belt formula, where μ is a constant. For the first term and the second term, values of the parameters $\boldsymbol{C}$, $\boldsymbol{D}$ and μ are experimentally identified. The third term denotes elastic forces due to bending motions of the flexible joint. This term can be analytically derived based on the preceding work[9] as follows:

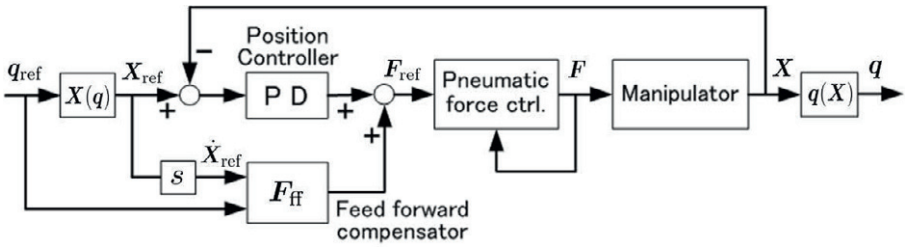

Fig.5 Block diagram of the position control system

$$\boldsymbol{K}(\boldsymbol{q}) = \boldsymbol{J}_{xq}(\boldsymbol{J}_{xq}^T\boldsymbol{J}_{xq})^{-1}\frac{\partial E}{\partial \boldsymbol{q}},$$

$$\boldsymbol{J}_{xq} = \begin{bmatrix} r\theta\sin\delta & -r\cos\delta \\ -r\theta\cos\delta & -r\sin\delta \\ -r\theta\sin\delta & r\cos\delta \\ r\theta\cos\delta & r\sin\delta \end{bmatrix} \tag{5}$$

$$E = \frac{1}{2}\theta^2\left(\frac{E_sI_s}{L} + \sum_{i=1}^{4}\frac{E_wI_w}{L - r\theta\cos\left(\frac{\pi}{2}(i-1)-\delta\right)}\right)$$

In equations (5), $\boldsymbol{J}_{xq}$ is a Jacobian matrix obtained from the time-derivative of equation (2), and E denotes the strain energy stored in the flexible joint where E_sI_s and E_wI_w denotes the bending stiffness of the machined spring and the super-elastic wires, respectively. Besides, effects of inertial forces and the gravitational force are neglected in this model.

The values of the parameters identified and used for the dynamic model are shown in Table 1. In this work, each value is the same for all of the four actuation DOFs.

Table 1. Values of the parameters used for the dynamic model

Parameter		Value
Viscous coefficient	$\boldsymbol{C}$	0.1 Ns/mm
Frictional force	$\boldsymbol{D}$	0.8 N
Frictional coefficient	μ	0.9
Bending stiffness of the spring	E_sI_s	4.2×10^{-4} Nm^2
Bending stiffness of the wires	E_wI_w	2.0×10^{-4} Nm^2

4. Position Control of the Flexible Wrist Joint

4.1. Design of the control system

Fig.5 shows the block diagram of the joint position control system. The system has a cascade controller consisting of the outer feedback loop for the position control and the inner feedback loop for the pneumatic force control.

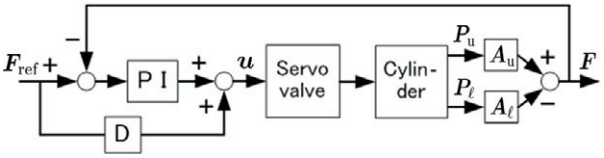

Fig.6 Block diagram of the pneumatic force control system

In the position control part, a PD controller for cylinder rod positions $\boldsymbol{X}$ is implemented to calculate reference values of pneumatic driving forces $\boldsymbol{F}_{ref}$. Moreover, a feed-forward compensation for the driving forces is added based on the dynamic model shown in equation (4). The pneumatic force control system is shown in Fig.6. In this part, a PI controller for pneumatic driving forces is implemented to calculate voltage inputs to the servo valves. Moreover, a feed-forward compensation using differential values of the references is added for the performance enhancement.

4.2. Joint position control experiment

Performances on the joint position control are evaluated through elementary experiments.

First, one-DOF bending motion of the wrist joint is performed with the following reference position inputs applied to the control system:

$$\begin{aligned} \delta_{ref} &= 0 \ \text{[deg]}, \\ \theta_{ref} &= 60\sin 0.6\pi t \ \text{[deg]} \end{aligned} \tag{6}$$

Fig.7 shows transient responses of some relevant control variables in this case. The results show a good control performance of the joint bending angle(θ) and its contributing cylinder positions(X_1, X_3). Seeing the response of pneumatic driving forces(F_1, F_3), amplitudes of driving forces become the same in a couple of push-and-pull actuations. Furthermore, nonlinear dynamics mainly caused by frictional forces are well-compensated by the controller.

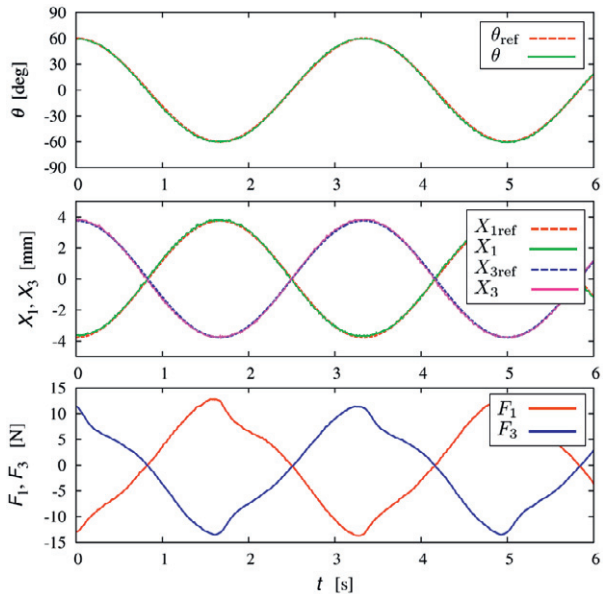

Fig.7 Experimental result of one-DOF bending motion control

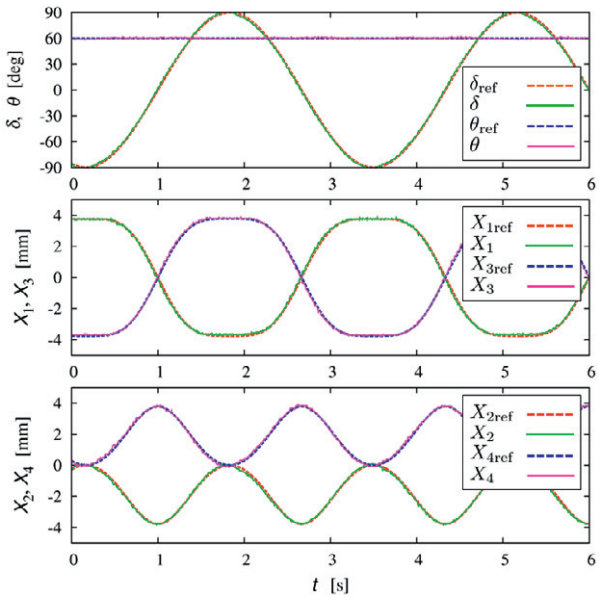

Fig.8 Experimental result of two-DOF combinational bending motion control

Next, a two-DOF combinational bending motion is performed. The reference position inputs are as follows:

$$\delta_{\mathrm{ref}} = 90\sin 0.6\pi t \ \ [\mathrm{deg}], \qquad \theta_{\mathrm{ref}} = 60 \ \ [\mathrm{deg}] \tag{7}$$

This motion realizes an axial rotation of the forceps tip maintaining the bending angle in combination with an axial rotation of the whole manipulator, which is especially useful for suturing task. Fig.8 shows transient responses of the joint positions and the cylinder positions in this case. The result shows a good control performance as in the case of the one-DOF bending motion.

According to the experimental results, controllability of the flexible wrist joint is considered acceptable for intuitive manipulations using a master-slave system.

5. Conclusions and Future Works

In this work, the authors developed a pneumatically-driven robotic forceps with a highly-simplified, 2-DOF bendable wrist mechanism. A machined spring is used for the joint structure, which is driven by push-pull actuations of super-elastic wires connected to pneumatic cylinders. The authors also designed the joint position controller based on the kinematic and dynamic models. The control performance is considered acceptable for intuitive manipulations using a master-slave system.

Our future works are to develop a method of external force estimation for the flexible wrist mechanism and to evaluate the manipulator performances in real surgical tasks through a master-slave operation.

References

[1] Thielmann, S., Seibold, U., Haslinger, R., Passig, G., Bahls, T., J¨org, S., Nickl, M., Nothhelfer, A., Hagn, U., Hirzinger, G., 2010. MICA - A new generation of versatile instruments in robotic surgery, Intelligent Robots and Systems (IROS), 2010 IEEE/RSJ International Conference on, p. 871-878.

[2] Bok, H. M., Ho, J. Y., 2012. Prototype Design of Robotic Surgical Instrument for Minimally Invasive Robot Surgery, Computer Aided Surgery, Vol. 3 of Proceedings in Information and Communications Technology, p. 20-28.

[3] Arata, J., Saito, Y., Fujimoto, H., 2010. Outer shell type 2 DOF bending manipulator using spring-link mechanism for medical applications, Robotics and Automation (ICRA), 2010 IEEE International Conference on, p. 1041-1046.

[4] Yoon, H. S., Oh, S. M., Jeong, J. H., Lee, S. H., Tae, K., Koh, K. C., Yi, B. J., 2011. Active bending endoscope robot system for navigation through sinus area, Intelligent Robots and Systems (IROS), 2011 IEEE/RSJ International Conference on, p. 967-972.

[5] Peirs, J., Reynaerts, D., Van Brussel, H., De Gersem, G., Tang, H. W., 2003. Design of an advanced tool guiding system for robotic surgery, Robotics and Automation (ICRA), 2003 IEEE International Conference on, Vol. 2, p. 2651-2656.

[6] Haraguchi, D., Tadano, K., Kawashima, K., 2011. A prototype of pneumatically-driven forceps manipulator with force sensing capability using a simple flexible joint, Intelligent Robots and Systems (IROS), 2011 IEEE/RSJ International Conference on, p. 931-936.

[7] Simaan, N., 2005. Snake-Like Units Using Flexible Backbones and Actuation Redundancy for Enhanced Miniaturization, Robotics and Automation (ICRA), 2005 IEEE International Conference on, p. 3012-3017.

[8] Li, H., Kawashima, K., Tadano, K., Ganguly, S., Nakano, S., 2011. Achieving Haptic Perception in Forceps' Manipulator Using Pneumatic Artificial Muscle, Mechatronics, IEEE/ASME Transactions on, Vol. PP, No. 99, p. 1-12.

[9] Xu, K., Simaan, N., 2008. An Investigation of the Intrinsic Force Sensing Capabilities of Continuum Robots, Robotics, IEEE Transactions on, Vol. 24, No. 3, p. 576-587.